

## On the mechanism of non-endosomal peptide-mediated cellular delivery of nucleic acids

Sébastien Deshayes, Sabine Gerbal-Chaloin, May C. Morris, Gudrun Aldrian-Herrada, Pierre Charnet, Gilles Divita, Frédéric Heitz\*

CRBM-CNRS, FRE 2593, 1919, route de Mende, 34293 Montpellier Cedex, France

Received 5 July 2004; received in revised form 21 September 2004; accepted 28 September 2004

Available online 7 October 2004

### Abstract

Recently, we described a new strategy for the delivery of nucleic acids into mammalian cells, based on an amphipathic peptide of 27 residues called MPG, which was designed on the basis of a hydrophobic domain derived from a fusion sequence associated with a nuclear localization sequence and separated by a linker. This peptide carrier constitutes a powerful tool for the delivery of nucleic acids in cultured cells, without requiring any covalent coupling. We have examined the conformational states of MPG in its free form and complexed with a cargo, as well as its ability to interact with phospholipids, and have investigated the structural consequences of these interactions. In spite of its similarity to the similarly designed cell-penetrating peptide Pep-1, MPG behaves significantly differently from the conformational point of view. Circular dichroism (CD) analysis reveals a transition from a nonstructured to a  $\beta$ -sheet conformation upon interaction with phospholipids. We propose that the membrane crossing process involves formation of a transient transmembrane pore-like structure. Partial conformational change of MPG is associated with formation of a complex with its cargo, and an increase in sheet content occurs upon association with the cell membrane.

© 2004 Elsevier B.V. All rights reserved.

**Keywords:** Cell-penetrating peptide; Conformation; Lipid–peptide interaction; Translocation mechanism

### 1. Introduction

The mechanism(s) underlying the delivery of therapeutics to subcellular compartments using cell penetrating peptides as carriers is still a matter of debate and sometimes controversial, in spite of numerous investigations. Besides the influence of experimental conditions which can affect the final localization of both carrier and cargo [1], it now appears clearly that the final cellular localization of a carrier peptide, associated or not to a cargo, depends on its sequence and thus most likely on its conformation [2–12]. In this context, we have developed a bipartite amphipathic peptide, called MPG, derived from the fusion peptide (FP)

of HIV1 gp41 associated with the nuclear localization signal (NLS) of SV40, which can act as efficient carrier and promote intracellular delivery of single- and double-stranded nucleic acids [13–16]. The internalization process is achieved through formation of a carrier/cargo complex and occurs through a non-endosomal pathway leading to a mainly nuclear final localization of the cargo. However, this localization can be affected by slight modifications in the NLS sequence, such as a K to S substitution, that lead to partial cytoplasmic release of the cargo, while no detectable effect can be observed on the free forms of the peptides [16,17]. The biological activities of the various cargos are in line with these observations. As an example, MPG promotes delivery of an siRNA thereby resulting in down-regulation of target mRNA. Knockdown activity is improved when the K-S mutant is used, due to greater delivery of the siRNA to the appropriate subcellular compartment for its activity [16,17]. However, little has been reported on the MPG-

\* Corresponding author. Tel.: +33 4 67 61 33 92; fax: +33 4 67 52 15 59.

E-mail address: [frederic.heitz@crbm.cnrs.fr](mailto:frederic.heitz@crbm.cnrs.fr) (F. Heitz).

mediated mechanism leading to cellular internalization of cargos. Indeed, up to now, conformational investigations dealing with MPG were restricted to studies in the absence of cargo [18]. The peptide was found to be non-ordered in water but to fold into a conformational state based on a  $\beta$ -sheet structure upon interacting with phospholipids. The peptide interacts strongly with phospholipids and hydrophobic interactions are the driving forces of the formation of peptide/lipid complexes [19].

In order to shed some light on this mechanism, we studied the influence of the cargo on the conformation of MPG, on the one hand, and of lipids on the other hand. These structural investigations were carried out in association with studies related to the ability of MPG to promote membrane permeabilization to ions and these properties can be related to the peptide-mediated translocation of the cargo through membranes.

## 2. Materials and methods

### 2.1. Peptide

G-A-L-F-L-G-F-L-G-A-A-G-S-T-M-G-A-W-S-Q-P-K-K-K-R-K-V peptide was synthesized as already described [20] on a Pioneer<sup>TM</sup> Peptide Synthesizer (Applied Biosystems, Foster City, CA) using a AEDI modified Expansin resin. It is *N*-acetylated and bears a cysteamide ( $-\text{NH}-\text{CH}_2-\text{CH}_2-\text{SH}$ ) group at its C-terminus. Peptide structure was identified by mass spectrometry and purity (about 99%) assessed by analytical HPLC.

### 2.2. Oligonucleotide

The *bcl-2* oligonucleotide [21] was obtained from MWG-Biotech (Courtaboeuf, France). The sequence of the antisense *bcl-2* oligonucleotide (*bcl-2* AS-ODN), which directs the translation initiation site of *bcl-2* transcripts, was 5'-TCTCCCAGCGTGC GCCAT-3. *bcl-2* AS-ODN-HEX was conjugated at its 3'-terminus with 6-carboxy-2',4,4',5',7,7'-hexachlorofluorescein.

### 2.3. Phospholipids

Dioleoylphosphatidylcholine (DOPC) and dioleoylphosphatidylglycerol (DOPG) were purchased from Avanti Polar Lipids (Alabaster, AL, USA).

### 2.4. Electromobility shift assay (EMSA)

Peptide was dissolved in water (100  $\mu\text{M}$ ) immediately before use. To form DNA/peptide complex, different amounts of peptide solution were added to 100 pmol of oligonucleotide to obtain charge ratios (negative charges of DNA versus positive charges of peptide) that ranged from 0 to 5. To complete complex formation, reaction mixtures

were incubated for 20 min at room temperature. The complexes were then loaded on a 1% TBE/agarose gel.

### 2.5. Fluorescence titration

Fluorescence experiments were performed using an SLM Series 2 luminescence spectrometer (Aminco Bowman). AS-ODN-HEX was excited at 525 nm, and the emission spectrum was recorded between 545 and 580 nm, with a spectral bandpass of 2 and 8 nm for excitation and emission, respectively. A fixed concentration of AS-ODN-HEX (10 nM) was titrated by increasing the concentration of MPG (in a range of 0–140 nM) at 25 °C in water.

For titration of the peptide by the oligonucleotide, the Trp residue was excited at 290 nm and the emission spectrum was recorded between 310 and 400 nm.

### 2.6. Fourier transform infrared (FTIR) spectroscopy

FTIR spectra were obtained on a Bruker IFS 28 spectrometer equipped with a liquid nitrogen cooled MCT detector. Spectra (1000 to 2000 scans) were recorded at a spectral resolution of 4  $\text{cm}^{-1}$  and were analyzed using the OPUS/IR2 program. Samples were obtained by deposition of solutions of lipid and peptide mixtures onto a fluorine plate where the solvents were allowed to evaporate under a nitrogen flux.

### 2.7. Circular dichroism (CD) measurements

CD spectra were recorded on a Jasco 810 dichrograph in a quartz cell with an optical path of 10 mm for aqueous solutions of peptide. The band positions were determined after smoothing the spectra by applying the method of Savitzky-Golay.

### 2.8. Electrophysiological recordings on *Xenopus laevis* oocytes

Ovaries were surgically removed from *X. laevis* females (Elevage de Lavalette, Montpellier, France) and oocytes were isolated after enzymatic dissociation (collagenase, type IA, Sigma, La Verpillere, France) and extensive washing, as already described [22]. After 24 h, oocytes were placed individually in a 50- $\mu\text{l}$  recording chamber. Macroscopic whole-cell currents were recorded under two electrode voltage-clamp using the GeneClamp 500 amplifier (Axon Instruments, Union City, CA) connected to the bath with the virtual-ground bath-clamp headstage and 3 M KCl agar-bridges. Voltage and current electrodes were filled with 3 M KCl and had a resistance of 1–2 M $\Omega$ . Junction potentials (typically less than 3–5 mV) were cancelled. Voltage-command, sampling, acquisition and analysis were performed with a Digidata 1200 and the pClamp program (version 6.01, Axon Instruments). All experiments were performed at room temperature (20–25 °C).

The recording solution had the following composition (in mM): NaCl, 100; HEPES, 10; MgCl<sub>2</sub>, 2; pH 7.2 with NaOH. MPG was applied directly to the bath at a final concentration of 10  $\mu$ M. Membrane current was recorded during voltage-ramps (−40 to +40 mV, 450 ms) applied from the holding potential of −80 mV every 5 s. Reversal potentials were measured as the zero-current potential after digital subtraction of traces recorded before and after peptide application.

### 3. Results and discussion

#### 3.1. Conformational studies of the free peptide in membrane and membrane-mimicking environments

In water, the far-UV CD spectrum of MPG exhibits a single minimum centered at 198 nm, which is typical of that expected for a nonstructured peptide [23]. Upon addition of phospholipid vesicles made of DOPG or DOPC/DOPG (80:20), drastic changes in the CD spectrum are observed. These modifications are mainly characterized by a severe decrease in the intensity of the negative band at 198 nm associated with a slight increase in the contribution centered at 223 nm (Fig. 1). Owing to the high wavelength position of the negative band, identification of the nature of the lipid-induced conformation is not straightforward. Therefore, it was achieved by comparison with the structural behavior of the peptide in the presence of SDS and by FTIR spectroscopy. The influence of SDS on the conformation was monitored by CD. As shown in Fig. 2, addition of SDS generates two different processes depending on the concentration of SDS in the medium. The first process, which is shown in Fig. 2a, occurs at low SDS concentrations (below  $2.2 \times 10^{-3}$  M) and can be interpreted as a random coil– $\beta$ -sheet transition. Indeed, the spectrum of MPG obtained in pure water is typical of that of a nonstructured peptide, while that at  $2.2 \times 10^{-3}$  M SDS suggests that the peptide

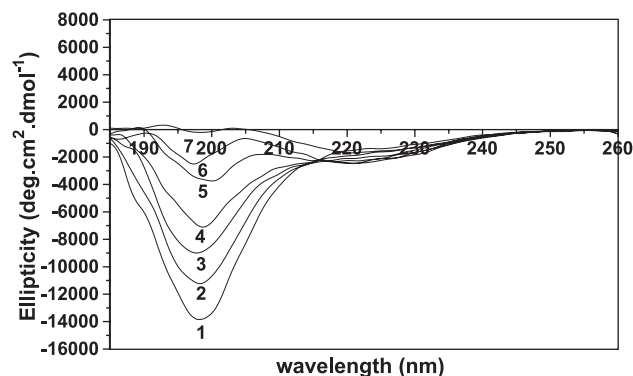


Fig. 1. Far-UV CD spectra of MPG in the presence of DOPG at various peptide/lipid ratios. Spectrum 1 corresponds to the pure peptide and spectra 2 to 7 to ratios 3.5, 1.8, 1.2, 0.9, 0.7 and 0.6, respectively. The spectra obtained for the DOPC/DOPG mixture are very similar and therefore are not shown.

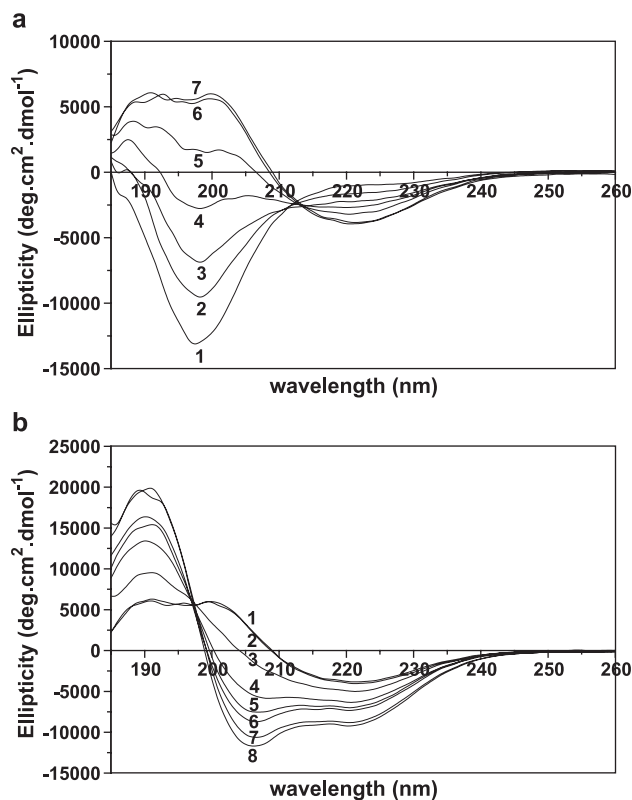


Fig. 2. Far-UV CD spectra of MPG in the presence of increasing amounts of SDS. (a) CD spectra for low content of SDS ( $< 2.2 \times 10^{-3}$  M); peptide concentration: 0.306 mg/ml. Spectra 1 to 7 correspond to 0,  $6 \times 10^{-5}$ ,  $1.3 \times 10^{-4}$ ,  $1.8 \times 10^{-4}$ ,  $2.4 \times 10^{-4}$ ,  $1.3 \times 10^{-3}$  and  $2.2 \times 10^{-3}$  M SDS, respectively. (b) CD spectra for high SDS contents; between  $2.2 \times 10^{-3}$  and  $13 \times 10^{-3}$ . Spectra 1 to 8 correspond to  $2.2 \times 10^{-3}$ ,  $3 \times 10^{-3}$ ,  $3.8 \times 10^{-3}$ ,  $4.3 \times 10^{-3}$ ,  $4.8 \times 10^{-3}$ ,  $5.7 \times 10^{-3}$ ,  $9 \times 10^{-3}$  and  $1.3 \times 10^{-2}$  M SDS, respectively.

adopts, at least in part, a sheet structure. In fact, because of the existence of an isodichroic point at 213 nm, it is likely that such a spectrum with one minimum (about 220 nm) and two maxima (190 and 202 nm) corresponds to a mixture of two structures which are  $\beta$ -sheet and random coil (about 60% and 40%, respectively) [24]. The latter probably arises from the lack of folding of the charged NLS sequence. As for the second process, which occurs at higher SDS concentrations, i.e., around the critical micellar concentration, it also concerns a conformational transition (SDS concentration  $4 \times 10^{-3}$  M). This transition is also characterized by the existence of an isodichroic point centered at 198 nm (Fig. 2b) and can be attributed to a transition from the abovementioned structural mixture to a form which is, at least in part, helical (one maximum around 192 nm and two minima at 206 and 222 nm), the NLS remaining unstructured.

Therefore, due to the strong similarity to the spectra detected at low concentration of SDS, the lipid-induced conformational change can be assigned to a conformational transition with formation of a sheet structure, at least in part, and rules out the existence of any helical structure. The existence of a sheet structure as the major structural

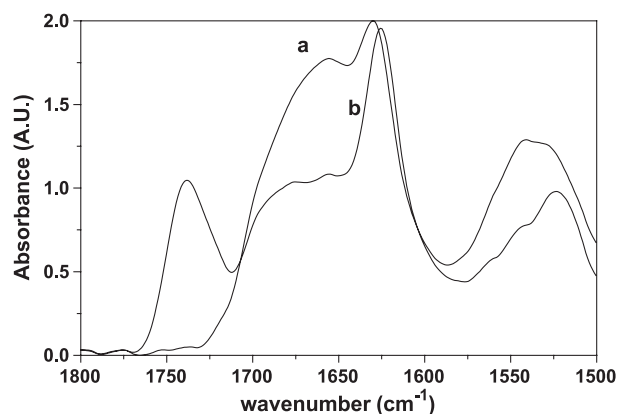


Fig. 3. FTIR spectrum of MPG in the absence (spectrum a) and in the presence (spectrum b) of DOPG at a peptide/lipid ratio of 1:9 (mol/mol).

component is confirmed by FTIR observations which reveal, in the presence of phospholipids, the existence of a major Amide I band around  $1625\text{ cm}^{-1}$  associated with a broad shoulder at  $1655\text{ cm}^{-1}$  (Fig. 3) [25]. On the basis of NMR data obtained in solution in water, with and without micelles of SDS [18], it can be stated that the hydrophobic sequence of the peptide corresponds to the folded domain while the remainder corresponding to the NLS is not structured.

### 3.2. Polynucleotide binding and induced conformational changes

#### 3.2.1. Binding

Two different approaches were used to monitor formation of a peptide/oligonucleotide complex. The first is based on spectroscopic measurements, namely fluorescence, while the second is based on gel shift assays.

- Fluorescence measurements. A 10 nM solution of HEX-labelled oligonucleotide (18-mer) was titrated with MPG. Changes in fluorescence intensity were monitored and are reported in Fig. 4, showing an abrupt linear decrease

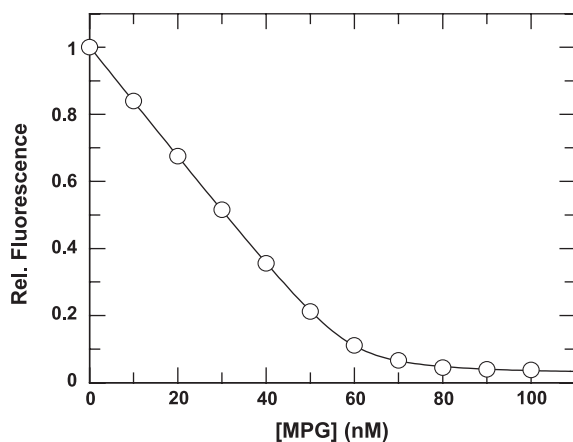


Fig. 4. Variation of the relative fluorescence (maximum of the emission spectrum) of HEX-labelled *bcl-2* oligonucleotide (solution containing 10 nmol) as a function of the amount of MPG peptide.

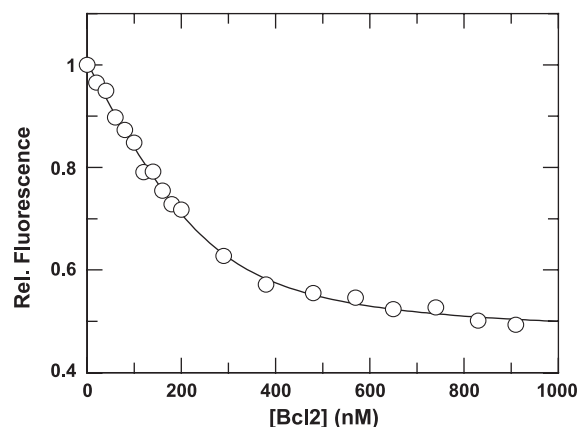


Fig. 5. Variation of the relative fluorescence (maximum of the emission spectrum) of MPG (solution containing  $2.5\text{ }\mu\text{mol}$ ) as a function of the amount of *bcl-2* oligonucleotide.

the extrapolation of which reveals a ratio of about 7 peptides per oligonucleotide. In terms of charges, this result indicates that the positive/negative charge ratio is 2 for the complex in good agreement with previous results obtained with a double-stranded DNA [26]. An identical stoichiometry for the complex was obtained by titration of the peptide by the oligonucleotide. Fig. 5 shows the variation of fluorescence intensity of the Trp residue of the carrier peptide. Extrapolation of the linear part of the titration curve leads to a complex built of a peptide/oligonucleotide ratio of 7.5, essentially similar to the value determined in the previous experiment. Moreover, determination of the equilibrium constants from both experiments indicates that the peptide exhibits high affinity for the oligonucleotide, respectively, 6 and 5 nM.

- Gel shift assays. In these experiments, oligonucleotide was incubated with the peptide at different peptide/oligonucleotide ratios and then submitted to gel migration. Fig. 6 shows the migration profiles obtained when the (+/−) charge ratio is varied from 0 to 5 (0 to 18 when expressed in molecular ratios). Clearly, for a charge ratio (+/−) of 1 or lower (lanes 1 to 3), the band corresponding to the free form of the oligonucleotide can be detected, while an increase of this ratio leads to disappearance of this band, accompanied by an increase in the amount of precipitated material remaining in the injection well.

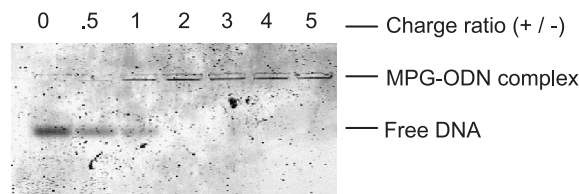


Fig. 6. Study of MPG-ODN complex stoichiometry by EMSA. ODN (100 pmol) was incubated with increasing concentration of MPG peptide corresponding to different charge ratios (+/−) from 0 to 5. After 20 min of incubation, complexes were electrophoresed on a 1% agarose gel, stained with EtBr and visualized under UV.



Taken together, these data indicate that the carrier peptide MPG strongly interacts with an oligonucleotide cargo to form a complex containing most probably more than 7 peptide molecules per oligonucleotide.

### 3.2.2. Induced conformational changes

Addition of the oligonucleotide to a solution of MPG in water in an oligonucleotide/peptide ratio ranging from 0 to 0.05 promotes changes in the CD spectrum. These changes include a decrease in the intensity of the negative band at 198 nm associated with a slight increase in the intensity of ellipticity in the 210–230-nm range (Fig. 7). These spectral variations indicate a decrease in the amount of unfolded peptide to the benefit of sheet structures as suggested by the increase in ellipticity around 223 nm. Interestingly, the CD spectra obtained for oligonucleotide/peptide ratios ranging from 0 to 0.1 indicate formation of a small but significant amount of  $\beta$ -sheet structure as revealed by the decrease in the intensity of the negative band at 198 nm associated with the small increase of the 223-nm contribution. The mixtures corresponding to the ratios previously used in transfection assays (0.1 or 0.2) [13,14,16,17] were used for further experiments related to the influence of phospholipids on the structure of the peptide engaged in a complex with oligonucleotide. Typical behavior is shown in Fig. 8 and reveals that addition of DOPG induces spectral variations that are similar to those observed in the absence of oligonucleotide, thereby indicative of formation of a  $\beta$ -sheet-based structure.

### 3.3. Peptide-induced ionic leakage

When the peptide (30  $\mu$ L of a 10  $\mu$ M peptide solution) in its free form or engaged in a complex at an oligonucleotide/peptide ratio of 0.1 was applied to voltage-clamped oocytes, marked increases in membrane

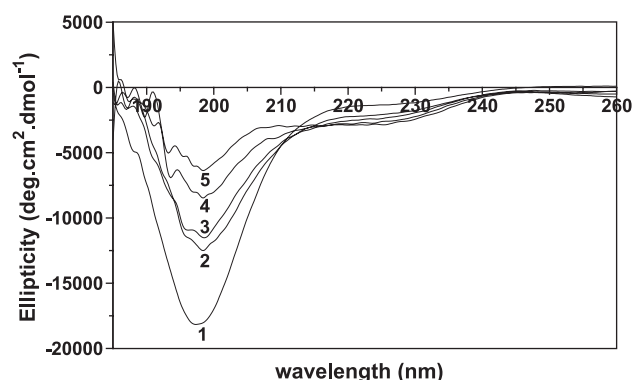


Fig. 7. Influence of various amounts of nucleic acids on the far-UV CD spectrum of MPG. The spectra shown here are those obtained after subtraction of the spectrum of the pure oligonucleotide. Spectrum 1 corresponds to the peptide without oligonucleotide. Spectra 2 to 5 correspond to peptide/oligonucleotide ratios (mole/mole) of 20, 15, 10 and 7.5, respectively.

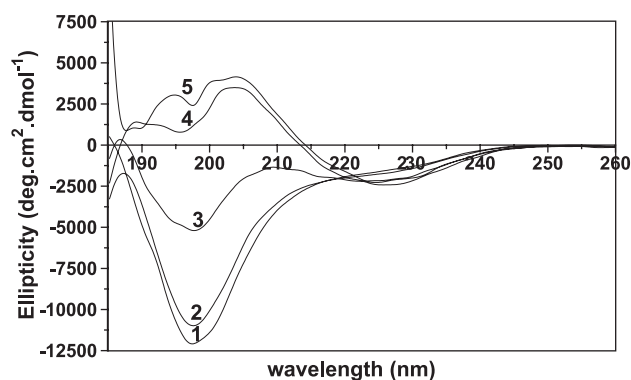


Fig. 8. Lipid-induced modifications of the far-UV CD spectrum obtained for a peptide/oligonucleotide ratio of 20. The oligonucleotide contribution was subtracted. Spectrum 1: without lipid; spectra 2 to 5 correspond to those obtained for peptide/lipid ratios of 4, 1, 0.33, and 0.16, respectively.

conductance were observed. These increases were visualized by increases in membrane currents recorded during voltage ramps applied from  $-40$  to  $+40$  mV (Fig. 9). The presence of nucleic acids has no effect on the reversal potential ( $-12$  mV) but appears to reduce the current amplitude. At this stage of the work, we cannot decide whether this decrease in the current arises from an artificial decrease of the peptide concentration because it is engaged in the complex, or to modification of the transmembrane current characteristics. Nevertheless, electrophysiological measurements, which strongly resemble those obtained for other channel-forming cell-penetrating peptides [22,28], suggest that the peptide-induced membrane permeabilization properties are due to formation of an ion channel. It must be mentioned that such conditions, which give rise to transmembrane currents, do not generate toxicity for the cells used for internalization experiments. That propidium iodide is not internalized under these conditions confirms the nontoxic effect of the peptide.

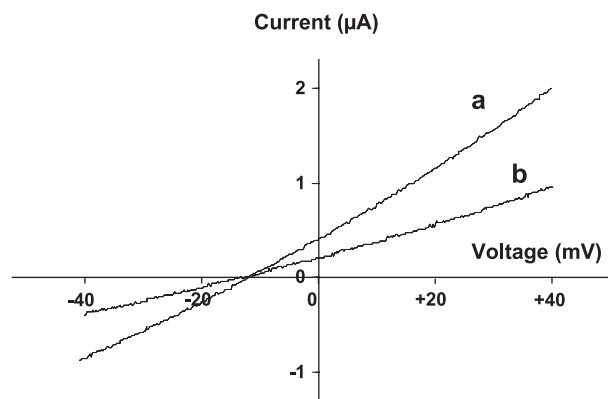


Fig. 9. Macroscopic current–voltage curve measured during application of MPG using a voltage-ramp from  $-40$  to  $+40$  mV. The current is shown after digital subtraction of leak current recorded before peptide application. The reversal potential is  $-12$  mV. Trace a corresponds to the current induced by the pure peptide while trace b was obtained using the peptide/oligonucleotide complex at a ratio of 10 (mol/mol).

### 3.4. The model accounting for translocation

Taking together all the structural information obtained so far for the vector peptide, whether associated or not with the cargo, a model for the membrane translocation process can be proposed. It is based on the following observations:

- The carrier peptide is not folded in the absence of cargo.
- The carrier peptide is not folded in the absence of membrane components.
- Partial folding of the carrier peptide into  $\beta$ -sheet occurs upon interaction with the cargo.
- The carrier peptide folds into a  $\beta$ -sheet structure upon interaction with membrane components such as phospholipids and can form complexes with phospholipids.
- When associated with the cargo, a more pronounced  $\beta$ -sheet folding is induced by phospholipids.
- The carrier, whether associated or not with a cargo, induces membrane permeability.
- The peptide strongly interacts with phospholipids with miscibility [29].

The model we propose to describe the translocation process is shown in Fig. 10 and follows four steps:

- Step 1. It corresponds to the formation of the peptide–cargo complex; here between the vector peptide and a double-stranded oligonucleotides. This association induces a partial folding of the hydrophobic domain of the peptide into a  $\beta$ -sheet structure.
- Step 2. It is associated to the uptake of the complex at the water–membrane interface at the external side of the cell. This uptake is accompanied by a complete  $\beta$ -sheet folding of the hydrophobic domain.
- Step 3. This step corresponds to the insertion of the complex into the membrane and formation of a pore-like structure based on the formation of a  $\beta$ -barrel type structure. The precise number of peptide molecules involved in the formation of this structure remains to be determined but is certainly higher than 8, for energetic reasons. The insertion is facilitated by the peptide–lipid interactions and the miscibility of the peptide with phospholipids.
- Step 4. The last step of the internalization process corresponds to the release of the peptide cargo complex into the cytoplasmic side of the cell. The internalized particle is still a complex but a partial decaging occurred since the vector peptide has a strong tendency to interact with phospholipids [19,29].

In conclusion, lipid-binding properties [17,18] associated with conformational investigations and electrophysiological measurements have led to the proposal of a model

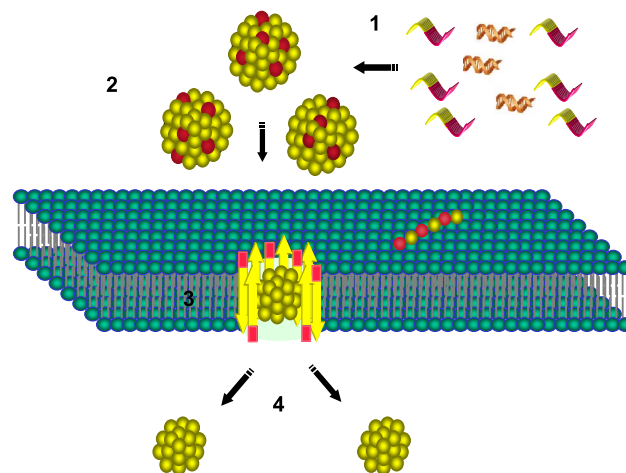


Fig. 10. Proposed schematic model for translocation of MPG/cargo complex through phospholipid bilayers (colour convention for the peptide: red corresponds to the NLS and yellow to the hydrophobic domain).

accounting for membrane translocation of MPG/cargo complexes. Comparison of this model with those proposed for other cell-penetrating peptides including Pep-1 [28] and cationic lipids [27] reveals several similarities. All are based on the formation of transient pore-like structures. However, a major difference between the two peptide-based models is that Pep-1-induced pore structure is based on the association of helical structures, while that induced by MPG is based on a  $\beta$ -sheet structure. Since Pep-1 favours the delivery of large peptides or proteins, but not nucleic acids, while MPG has the opposite behavior, the next question to be addressed is whether this conformational difference between the two peptide vectors governs the nature of the cargo that is delivered into cells. Further studies are required to address this issue and are presently in progress in our laboratory.

### Acknowledgments

This work was supported by the EU, grant QLK2-CT-2001-01451.

### References

- [1] J.P. Richard, K. Melikov, E. Vives, C. Ramos, B. Verbeure, M.J. Gait, L.V. Chernomordik, B. Lebleu, Cell-penetrating peptides. A reevaluation of the mechanism of cellular uptake, *J. Biol. Chem.* 278 (2003) 585–590.
- [2] R.I. Mahato, Non-viral peptide-based approaches to gene delivery, *J. Drug Target.* 7 (1999) 249–268.
- [3] S. Gottschalk, J.T. Sparrow, J. Hauer, M.P. Mims, F.E. Leland, S.L. Woo, L.C. Smith, A novel DNA–peptide complex for efficient gene transfer and expression in mammalian cells, *Gene Ther.* 3 (1996) 48–57.
- [4] T.B. Wyman, F. Nicol, O. Zelphati, P.V. Scaria, C. Plank, F.C. Szoka Jr., Design, synthesis, and characterization of a cationic peptide that binds to nucleic acids and permeabilizes bilayers, *Biochemistry* 36 (1997) 3008–3017.

- [5] J. Gariépy, K. Kawamura, Vectorial delivery of macromolecules into cells using peptide-based vehicles, *Trends Biotechnol.* 19 (2001) 21–28.
- [6] K. Rittner, A. Benavente, A. Bompert-Sorlet, F. Heitz, G. Divita, R. Brasseur, E. Jacobs, New basic membrane-destabilizing peptides for plasmid-based gene delivery in vitro and in vivo, *Molec. Ther.* 5 (2002) 104–114.
- [7] R. Cartier, R. Reszka, Utilization of synthetic peptides containing nuclear localization signals for nonviral gene transfer systems, *Gene Ther.* 9 (2002) 157–167.
- [8] M. Lindgren, M. Hällbrink, A. Prochiantz, Ü. Langel, Cell-penetrating peptides, *Trends Pharmacol. Sci.* 21 (2000) 99–103.
- [9] J.S. Wadia, S.F. Dowdy, Protein transduction technology, *Curr. Opin. Biotechnol.* 13 (2002) 52–56.
- [10] G. Dom, C. Shaw-Jackson, C. Matis, O. Bouffieux, J.J. Picard, A. Prochiantz, M.P. Mingot-Leclercq, R. Brasseur, R. Rezsöházy, Cellular uptake of Antennapedia Penetratin peptides is a two-step process in which phase transfer precedes a tryptophan-dependent translocation, *Nucleic Acids Res.* 31 (2003) 556–561.
- [11] R. Truant, B.R. Cullen, The arginine-rich domains present in human immunodeficiency virus type 1 Tat and Rev function as direct importin beta-dependent nuclear localization signals, *Mol. Cell. Biol.* 19 (1999) 1210–1217.
- [12] C. Rudolph, C. Plank, J. Lausier, U. Schillinger, R.H. Müller, J. Rosenecker, Oligomers of the arginine-rich motif of the HIV-1 TAT protein are capable of transferring plasmid DNA into cells, *J. Biol. Chem.* 278 (2003) 11411–11418.
- [13] M.C. Morris, P. Vidal, L. Chaloin, F. Heitz, G. Divita, A new peptide vector for efficient delivery of oligonucleotides into mammalian cells, *Nucleic Acids Res.* 25 (1997) 2730–2736.
- [14] M.C. Morris, L. Chaloin, J. Méry, F. Heitz, G. Divita, A novel potent strategy for gene delivery using a single peptide vector as a carrier, *Nucleic Acids Res.* 27 (1999) 3510–3517.
- [15] M.C. Morris, L. Chaloin, F. Heitz, G. Divita, Translocating peptides and proteins and their use for gene delivery, *Curr. Opin. Biotechnol.* 11 (2000) 461–466.
- [16] F. Simeoni, M.C. Morris, F. Heitz, G. Divita, Insight into the mechanism of the peptide-based gene delivery system MPG: implications for delivery of siRNA into mammalian cells, *Nucleic Acids Res.* 31 (2003) 2717–2724.
- [17] S. Deshayes, N. Van Mau, M.C. Morris, G. Divita, F. Heitz, Structural requirements for non-covalent peptide-mediated cellular delivery of siRNAs, in: M. Chorev, T.K. Sawyer (Eds.), *Proceedings of the 18th American Peptide Symposium*, American Peptide Society, San Diego, 2004, pp. 802–804.
- [18] P. Vidal, L. Chaloin, A. Heitz, N. Van Mau, J. Méry, G. Divita, F. Heitz, Interactions of primary amphipathic vector peptides with membranes. Conformational consequences and influence on cellular localization, *J. Membr. Biol.* 162 (1998) 259–264.
- [19] Y. Li, F. Heitz, C. Le Grimmellec, R.B. Cole, Hydrophobic component in noncovalent binding of fusion peptides to lipids as observed by electrospray mass spectrometry, *Rapid Commun. Mass Spectrom.* 18 (2004) 135–137.
- [20] P. Vidal, L. Chaloin, J. Méry, N. Lamb, N. Lautredou, R. Bennes, F. Heitz, Solid-phase synthesis and cellular localization of a C- and/or N-terminal labelled peptide, *J. Pept. Sci.* 2 (1996) 125–133.
- [21] A. Webb, D. Cunningham, F. Cotter, P.A. Clarke, F. di Stefano, P. Ross, M. Corbo, Z. Dziewanowska, BCL-2 antisense therapy in patients with non-Hodgkin lymphoma, *Lancet* 349 (1997) 1137–1141.
- [22] L. Chaloin, E. Dé, P. Charnet, G. Molle, F. Heitz, Ionic channels formed by a primary amphipathic peptide containing a signal peptide and a nuclear localization sequence, *Biochim. Biophys. Acta* 1375 (1998) 52–60.
- [23] G.D. Fasman (Ed.), *Circular Dichroism and the Conformational Analysis of Biomolecules*, Plenum Press, New York, 1996.
- [24] N. Greenfield, G.D. Fasman, Computed circular dichroism spectra for the evaluation of protein conformation, *Biochemistry* 8 (1969) 4108–4116.
- [25] F. Dousseau, M. Pezolet, Determination of the secondary structure content of proteins in aqueous solutions from their amide I and amide II infrared bands. Comparison between classical and partial least-squares methods, *Biochemistry* 29 (1990) 8771–8779.
- [26] E. Marthinet, G. Divita, J. Bernaud, D. Rigal, L.G. Baggetto, Modulation of the typical multidrug resistance phenotype by targeting the MED-1 region of human MDR1 promoter, *Gene Ther.* 7 (2000) 1224–1233.
- [27] A. Chanturiya, J. Yang, P. Scaria, J. Stanek, J. Frei, H. Mett, M. Woodle, New cationic lipids form channel-like pores in phospholipid bilayers, *Biophys. J.* 84 (2003) 1750–1755.
- [28] S. Deshayes, A. Heitz, M.C. Morris, P. Charnet, G. Divita, F. Heitz, Insight into the mechanism of internalization of the cell-penetrating carrier peptide Pep-1 through conformational analysis, *Biochemistry* 43 (2004) 1449–1457.
- [29] S. Deshayes, T. Plénat, G. Aldrian-Herrada, G. Divita, C. Le Grimmellec, F. Heitz, Primary amphipathic cell-penetrating peptides: structural requirements and interactions with model membranes, *Biochemistry* 43 (2004) 7698–7706.